# At Critically Low Antigen Densities, IgM Hexamers Outcompete Both IgM Pentamers and IgG1 for Human Complement Deposition and Complement-Dependent Cytotoxicity

Oskam, N.; Ooijevaar-de Heer, P.; Derksen, N.I.L.; Kruithof, S.; Taeye, S.W. de; Vidarsson, G.; ... ; Rispens, T.

# At Critically Low Antigen Densities, IgM Hexamers Outcompete Both IgM Pentamers and IgG1 for Human Complement Deposition and Complement-Dependent Cytotoxicity

**Nienke Oskam,* Pleuni Ooijevaar-de Heer,* Ninotska I. L. Derksen,* Simone Kruithof,* Steven W. de Taeye,† Gestur Vidarsson,† Sanne Reijm,‡ Theresa Kissel,‡ René E. M. Toes,‡ and Theo Rispens***

**IgM is secreted as a pentameric polymer containing a peptide called the joining chain (J chain). However, integration of the J chain is not required for IgM assembly and in its absence IgM predominantly forms hexamers. The conformations of pentameric and hexameric IgM are remarkably similar with a hexagonal arrangement in solution. Despite these similarities, hexameric IgM has been reported to be a more potent complement activator than pentameric IgM, but reported relative potencies vary across different studies. Because of these discrepancies, we systematically investigated human IgM-mediated complement activation. We recombinantly generated pentameric and hexameric human IgM (IgM+J and IgM−J, respectively) mAbs and measured their ability to induce complement deposition and complement-dependent cytotoxicity when bound to several Ags at varying densities. At high Ag densities, hexameric and pentameric IgM activate complement to a similar extent as IgG1. However, at low densities, hexameric IgM outcompeted pentameric IgM and even more so IgG1. These differences became progressively more pronounced as antigenic density became critically low. Our findings highlight that the differential potency of hexameric and pentameric IgM for complement activation is profoundly dependent on the nature of its interactions with Ag. Furthermore, it underscores the importance of IgM in immunity because it is a more potent complement activator than IgG1 at low Ag densities.** ***The Journal of Immunology*****, 2022, 209: 16–25.**

Immunoglobulin M is the first Ab to be expressed both in ontogeny and in the immune response. It is initially expressed on immature B cells as a monomeric membrane-bound receptor anchored by its C-terminal transmembrane domain. Secreted IgM is instead produced with a hydrophilic tailpiece that induces polymerization of the Ab and drives association with a small, 15-kDa protein called the joining chain (J chain). In the presence of this J chain, polymeric IgM assembles as a pentamer consisting of five IgM protomers (H2L2) linked by a single J chain (1–3).

Regardless, integration of J chain is not required for polymerization or secretion of IgM. When IgM is expressed in the absence of J chain, it can instead be replaced by an additional IgM protomer so the polymeric IgM assembles as a hexamer (Fig. 1A). J chain–negative IgM is not exclusively assembled as a hexamer, and varying amounts of smaller polymers, most commonly pentamers, have been reported to be secreted as well (4–9).

Functionally, IgM, as well as IgG, can activate the classical pathway of the complement system by interacting with C1q, which leads to activation of the complement cascade and downstream assembly of the membrane attack complex and eventually cell lysis (Fig. 1B). IgM can bind its Ag with both Fab arms and takes on a dome-shaped conformation (10, 11), after which C1q interacts with residues exposed in the Fc region. Recent studies demonstrate that the structures of pentameric and hexameric IgM are remarkably similar, also when bound to Ag, with the pentamer adopting a conformation resembling a hexamer with one "leg" missing (10, 12–14). A hexameric conformation also plays an important role for complement activation by IgG1, which on Ag binding preferably forms hexamers via Fc–Fc interactions to interact with C1q (15, 16).

Despite the similarities through which these Abs interact with C1q, they do not always activate complement to the same extent; generally, IgM is considered a more potent complement activator than IgG1 (17–19). Polymerization of IgM has been shown to be a requirement for complement activation because IgM monomers are not able to do so (20). It is therefore also conceivable that the polymerization state of IgM also influences its activating potency. Indeed, multiple studies reported that hexameric IgM activates complement at least three times, but sometimes up to 100 times more efficiently than pentameric IgM (4, 21–25). However, it should be noted that these large differences are found when using guinea pig serum rather than human serum, for which the differences are reported to be much smaller and variable (4, 6, 24). Overall, the role of the degree of IgM polymerization (i.e., hexamer versus pentamer) in C1q binding and complement activation remains uncertain.

Therefore, in this study, we sought to systematically investigate complement activation by IgM hexamers (−J) and pentamers (+J)

*Department of Immunopathology, Sanquin Research and Landsteiner Laboratory, Academic Medical Center, Amsterdam, the Netherlands; †Department of Experimental Immunohematology, Sanquin Research and Landsteiner Laboratory, Academic Medical Center, Amsterdam, the Netherlands; and ‡Department of Rheumatology, Leiden University Medical Center, Leiden, the Netherlands

ORCIDs: 0000-0002-7388-2572 (P.O.-d.H.); 0000-0002-0189-2675 (N.I.L.D.); 0000-0001-5621-003X (G.V.); 0000-0002-4424-4256 (S.R.); 0000-0002-5749-8087 (T.K.); 0000-0002-9618-6414 (R.E.M.T.).

Received for publication December 23, 2021. Accepted for publication April 21, 2022.

This work was supported by Dutch Arthritis Foundation Grant 17-2-404.

Address correspondence and reprint requests to Nienke Oskam, Sanquin Research, Plesmanlaan 125, 1066 CX Amsterdam, the Netherlands. E-mail address: n.oskam@sanquin.nl

The online version of this article contains supplemental material.

Abbreviations used in this article: ACPA, anti-citrullinated protein Ab; bt, biotin; CDC, complement-dependent cytotoxicity; HSA, human serum albumin; HSA-bt, biotinylated HSA; J chain, joining chain; MALS, multiangle laser light scattering.

using well-defined, monoclonal preparations of IgM with and without J chain. In particular, the effect of Ag density was investigated (Fig. 1C, 1D). We show that whereas hexameric and pentameric IgM have similar potencies at a high Ag density, the relative potency of hexamers can be vastly larger compared with pentamers or IgG1 at low densities.

## Materials and Methods

### *Abs*

To detect deposition of complement components in ELISA, we used anti–C3–19 (26), anti–C4–10 (27), and anti–C1q-2 (28), which were HRP labeled using a HRP Conjugation Kit (Abcam). Mouse anti-IgM (MH-15; Sanquin), a J chain (MCA693; Bio-Rad), and goat anti-mouse IgG-HRP (GM-17; Sanquin) were used to visualize IgM on Western blot.

### *Production of recombinant Abs*

Synthetic constructs coding the constant domains of human IgM and κ with different variable domains, as well as J chain, were cloned into pcDNA3.1 expression vectors (GeneArt; Invitrogen). The Abs produced were specific for biotin (bt) (29, 30), citrullinated proteins (anti-citrullinated protein Ab [ACPA] clones 2D5 and 1G8) (31), G1m(a) (anti-a) (32), and IgG-Fc (rheumatoid factors RF-61 [33] and RF-AN [34, 35]). The anti-bt Ab was also produced as human IgG1. Only the rheumatoid factors and the ACPAs were originally human IgM.

Abs were produced analogously as described previously (36) under serum-free conditions (FreeStyle 293 expression medium; Invitrogen) by cotransfecting relevant H chain–, L chain–, and J chain–expressing vectors in HEK293F cells using PEI-MAX according to the manufacturer's instructions (Invitrogen). The cells were cultured at 37°C, 8% $CO_2$, while shaking at 125 rpm. At day 5 of transfection, the cultures were centrifuged, and supernatant was harvested and filtered over a syringe filter with a pore size of 0.20 μm (Whatman Puradisc 30; Sigma-Aldrich). IgG1 was loaded on a HiTrap protG column (GE Healthcare) and eluted with 0.1 M glycine (pH 2.5–3). The eluate was immediately neutralized with 2 M Tris–HCl (pH 9).

For the purification of IgM, 3 mg RPLGal1 (Glycoselect) was coupled to 100 mg CNBr-activated Sepharose 4B (GE Healthcare) according to the manufacturer's protocol. Before purification the column was activated with 1× TBS (10 mM Tris, 140 mM NaCl, 0.1 mM $CaCl_2$ [pH 7.4]) supplemented with 1 mM $CaCl_2$, $MgCl_2$, and $MnCl_2$. The culture supernatant, also supplemented with 1 mM $CaCl_2$, $MgCl_2$, and $MnCl_2$, was loaded onto the column and eluted with 0.5 M galactose in 1× TBS. The eluates were dialyzed against 5 mM NaAc (pH 4.5) for IgG1 and 20 mM NaAc, 300 mM NaCl (pH 5.5) for IgM, and concentrated by multiple rounds of centrifugation using a 10-kDa spin column (Amicon Utra-4 Centrifugal Filter Unit; Merck). The concentration of the purified Igs was determined by measuring absorbance at 280 nm (NanoDrop One; Thermo Fischer Scientific), and the samples were aliquoted and stored at −20°C.

### *Characterization of IgM*

To assess quality and purity of the produced monoclonal IgMs, 50 μg of each monoclonal was fractionated using HP-SEC Agilent 1260 Infinity II (Agilent Technologies) with a Superose 6 Increase 10/300 GL Column (GE Healthcare). Elution was monitored by measuring the absorption at 280 nm. The anti-bt clone was run in PBS with added 0.3M NaCl to prevent it from sticking to the column. The m.w. of peaks was determined from monitoring multi-angle laser light scattering (MALS) using a mini-DAWN (Wyatt Technology Europe) and refractive index using an Optilab (Wyatt Technology Europe), and calculated using a refractive index increment of 0.185 (ml/g), and a second virial coefficient of 0 using the Astra software (version 7.3.2; Wyatt Technology Europe). The calculation of the m.w. was based on the Zimm equation (37, 38).

IgM was further visualized on 3–8% Tris-Acetate Protein Gels and pH 3–10 IEF Gels (NuPAGE; Invitrogen) according to the manufacturer's protocol. Gels were stained with Coomassie (InstantBlue; Expedeon) for at least 30 min. For Western blot analysis, samples were run on 4–12% Bis-Tris Protein Gels (NuPAGE; Invitrogen) according to the manufacturer's protocol under reducing conditions. Proteins were transferred to a nitrocellulose membrane (iBlot transfer system; Thermo Fischer) and detected with mouse anti–IgM-HRP or mouse anti–J chain and goat anti-mouse Ig-HRP. The blot was developed with Pierce ECL Western blotting Substrate (Thermo Fisher Scientific) according to the manufacturer's protocol.

### *Biotinylation of human serum albumin*

Human serum albumin (HSA; Albuman; Sanquin) was first depleted of IgG by incubation with protG Sepharose. IgG-depleted HSA was then biotinylated. We used a biotinylation reagent without a linker (EZ-Link Sulfo-NHS-bt; Thermo Fischer Scientific), with a short linker (EZ-Link Sulfo-NHS-LC-bt; Thermo Fischer Scientific), and with a long linker (EZ-Link Sulfo-NHS-LC-LC-bt; Thermo Fischer Scientific). HSA (1 mg/ml) was incubated with different concentrations of these biotinylation reagents for 2 h at room temperature in PBS and subsequently dialyzed to PBS overnight with a 10-kDa cassette to remove any unbound reagent. The amount of bt per HSA molecule, the biotinylation degree, was determined for each batch as described previously (39).

### *Complement deposition ELISAs*

The ability of the monoclonal Igs to activate complement was determined in ELISAs as described previously (40), but with some modifications. To study activation by ACPA IgMs, fibrinogen (IgG and C4 depleted) was citrullinated using rabbit skeletal muscle protein arginine deiminase (Sigma) and coated at 10 μg/ml in PBS. Alternatively, varying concentrations of cfib2-bt peptide [bt-SGSGCCitPAPPPISGGGYCitACit] (41) or CCP4-bt peptide [bt-HQFRFCitGNleSRAACZO] (42) were incubated for an hour on streptavidin-coated plates (Thermo Fischer Scientific) at room temperature. For the anti-bt Abs, biotinylated HSA (HSA-bt) was used as a coat. HSA-bt was diluted to 5 μg/ml in PBS and coated overnight at 4°C on MaxiSorp plates (Thermo Fisher Scientific). Abs were diluted in PBS with 0.1% Tween 20 and 0.002% w/v gelatin (PTG). Veronal buffer (3 mM Barbital, 1.8 mM sodium-Barbital, 0.146 M NaCl) was supplemented with 2.5–50% of a normal human serum pool and 1 mM $CaCl_2$ and 0.5 mM $MgCl_2$. The deposited C1q, C3b, or C4b was detected with the respective mouse HRP-conjugated Abs. Detection was visualized with 3,3′,5,5′-tetramethylbenzidine (100 μg/ml) in 0.11 M acetate buffer (pH 5.5) containing 0.003% $H_2O_2$ (Merck), and the reaction was stopped with 0.2 M $H_2SO_4$. The OD was read at 450 and 540 nm for background correction using a BioTek microtiter plate reader.

### *Complement-dependent cytotoxicity assay*

The hemolytic activity of the anti-bt recombinant Abs was determined in a complement-dependent cytotoxicity (CDC) assay as described previously (40), but with some minor alterations. Healthy donor EDTA blood with blood group O was used for all experiments. After three rounds of washing with PBS, 100 μl of packed RBCs was resuspended in 700 μl PBS containing varying amounts of biotinylation reagent and incubated in the dark at room temperature for at least 60 min. After three washes, RBCs were diluted to ∼6 ml in veronal buffer supplemented with 0.05% w/v gelatin. A total of 35 μl RBC suspension was added to 65 μl veronal buffer supplemented with 0.05% w/v gelatin, 1 mM $CaCl_2$, 0.5 mM $MgCl_2$, 10% of a normal human serum pool, and anti-bt Abs. The suspension was incubated at 37° while shaking for at least 90 min. For the 100% lysis control, 65 μl water was added to the 35 μl cell suspension. After incubation, 50 μl PBS was added to each well to increase the volume slightly, plates were centrifuged for 2 min at 1800 rpm, and 100 μl supernatant was transferred to flat-bottom MaxiSorp plates. The OD was read at 412 and 690 nm for background correction. The percentage of lysis was calculated as (OD sample/OD 100% lysis) × 100.

## Results

### *Production of recombinant IgM with and without J chain*

To study complement activation by polymeric IgM in more detail and in a controlled system, we produced recombinant human IgM with three different specificities, two ACPAs (clones 2D5 and 1G8) and an anti-bt Ab (of mouse origin but with human constant domains). IgM was purified from culture supernatants with a lectin column that binds to glycans on IgM and was mildly eluted with galactose (Fig. 1). We found this allowed efficient purification with minimal degradation and aggregation of the Abs.

These clones, as well as three control IgM clones, were analyzed with size-exclusion chromatography combined with MALS (Fig. 2A, Supplemental Fig. 1) and on native protein gel (Fig. 2B). Not all clones entered the gel, however; because analysis by HP-SEC showed that these clones eluded in single peaks, we can conclude that this is not due to aggregation. The estimated m.w. as determined by MALS

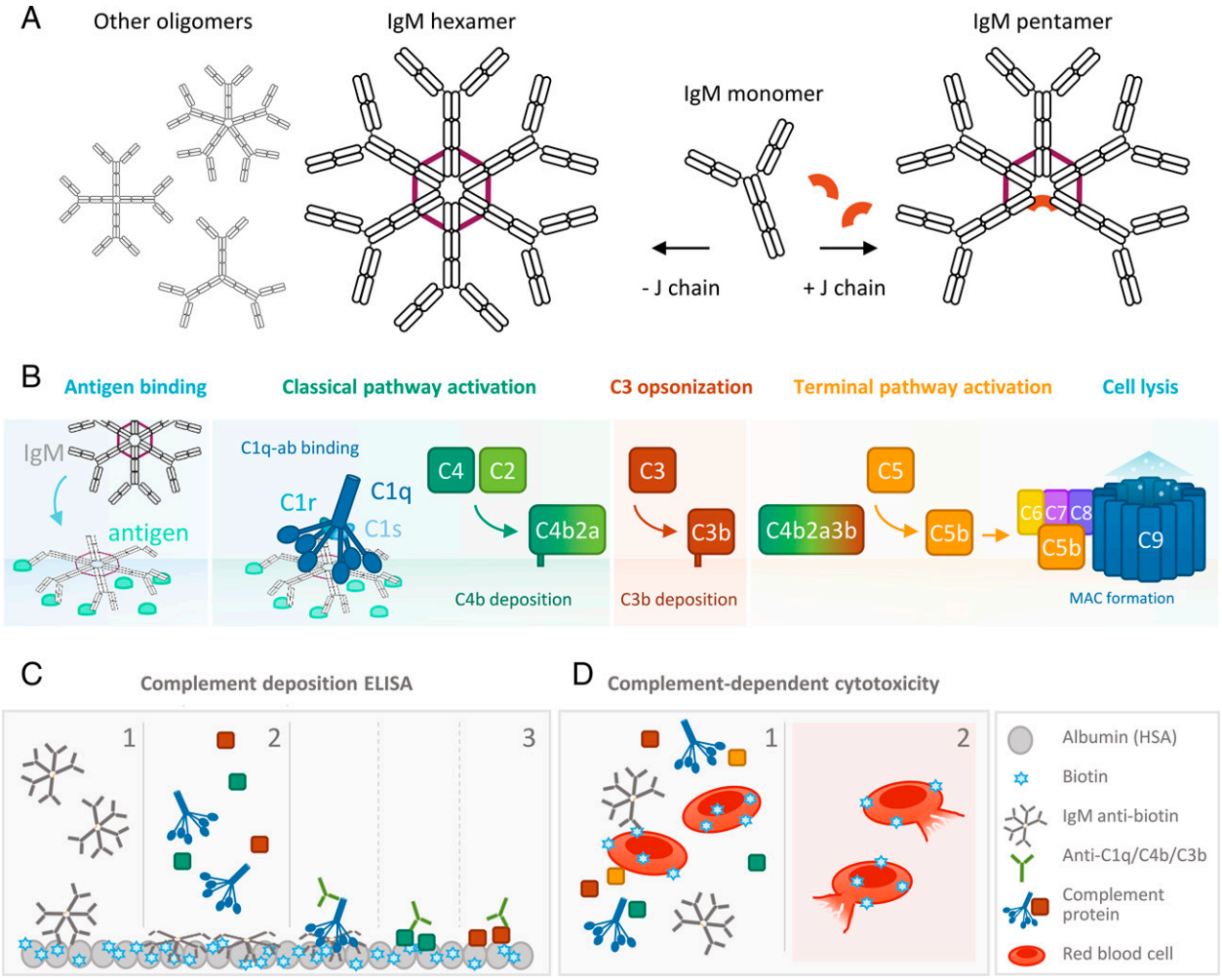


**FIGURE 1.** IgM polymerization and complement activation. (**A**) Schematic representation of polymeric IgM. In the presence of J chain, IgM is assembled as a pentamer, which takes on a hexagonal arrangement, with J chain taking the position of the last missing arm (as depicted on the right). In absence, however, IgM will predominantly form hexamers, but smaller oligomers also occur (as depicted on the left). (**B**) Classical pathway activation by IgM is initiated by Ag binding and subsequent recognition of IgM by C1q. An activated C1 complex will cleave C4 and C2, to form the C3 convertase C4bC2a, which in turn cleaves C3 and causes C3b deposition on the cell surface. The C5 convertase (C4bC2aC3b) is formed, and the terminal pathway is activated through cleavage of C5, followed by the recruitment of C6–9, the formation of the membrane attack complex, and eventual cell lysis. (**C**) To determine deposition of classical pathway components by IgM in ELISA, a matched set of anti-bt antibodies was allowed to bind to biotinylated albumin-coated plates (C1) and subsequently incubated with 2.5% of human serum (C2) to activate the classical pathway. Bound C1q, C4b, and C3b were detected with specific HRP-conjugated antibodies (C3). (**D**) Terminal pathway activation by IgM antibodies was studied in a CDC assay. Healthy O-donor RBCs were biotinylated and incubated with anti-bt antibodies and 10% of human serum (D1). Sufficient opsonization of cells leads to cell lysis (D2), which is then measured as the absorbance of hemoglobin in the suspension supernatant.

analysis indicates that IgM−J assembles as a larger multimer than IgM+J for every clone and correlates to expected molecular weights of hexameric and pentameric IgM, respectively. Taken together, this confirms that J chain–containing IgM adapts a pentameric configuration, whereas in the absence of J chain, IgM predominantly forms hexamers. These results were further supported by visualization of IgM preparations on an isoelectric focusing gel (Supplemental Fig. 1A). Western blot confirmed the presence and absence of the J chain for IgM+J and IgM−J, respectively (Supplemental Fig. 1B).

Later we will refer to IgM+J as pentameric IgM and to IgM−J as hexameric IgM.

*Complement activation by IgM autoantibodies is driven by Ag density*

Our initial experiments focused on complement activation by a monoclonal IgM autoantibody based on BCR sequences isolated from a rheumatoid arthritis patient, i.e., an ACPA. Although we are not aware of any data on the polymerization state of these Abs in vivo, we chose to produce the IgM ACPA (2D5) both with and without J chain and tested their ability to activate complement when bound to citrullinated fibrinogen as an Ag.

For both IgM isomers, we could measure only very little to no C1q binding (Fig. 3A). Surprisingly, we found that hexameric IgM is capable of activating complement in this setting, while we found almost no complement activation for pentameric IgM, as assessed by measuring C4b/C3b deposition (Fig. 3A). We hypothesized that this was due to the nature of the Ag used, and therefore we decided to switch to Ags that would allow us better control of the density. To this end, we repeated the assay with two synthetic citrullinated peptides: cfib2, a 20-aa citrullinated fibrinogen peptide; and CCP4, a 15-aa cyclic citrullinated peptide (Fig. 3B).

Interestingly, with these synthetic peptides as Ags, we observed a pronounced effect of Ag density for ACPA 2D5 pentameric versus hexameric IgM to activate complement. In the case of cfib2, we even found that with higher Ag densities, the pentamer and hexamer activate complement similarly, while the differences

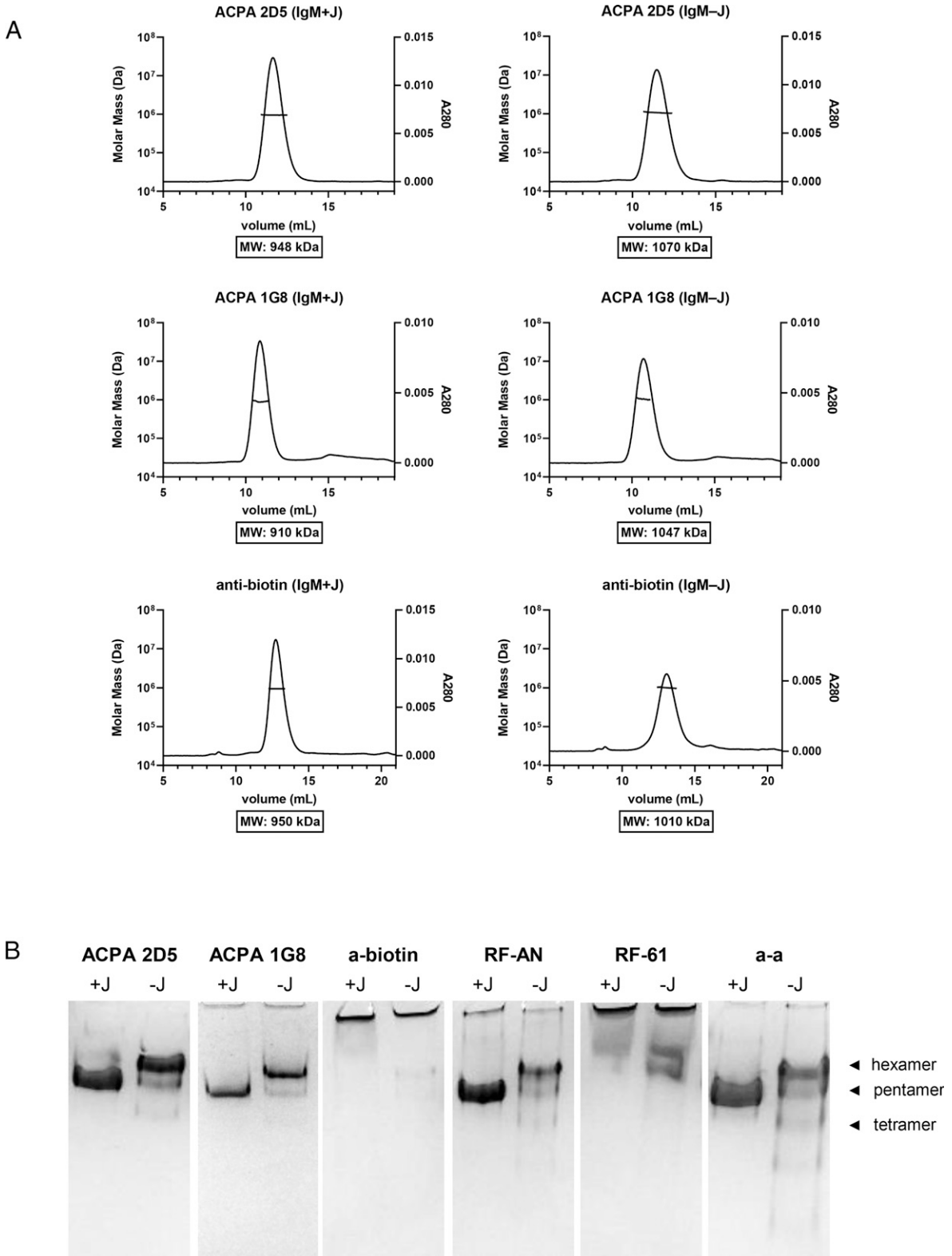


**FIGURE 2.** Characterization of monoclonal IgM with and without J chain. Monoclonal IgM antibodies were produced in the presence (IgM+J) and absence (IgM–J) of J chain and characterized with HP-SEC combined with MALS (**A**) and native PAGE (**B**). (A) Elution profiles (right *y*-axis) and estimated molecular mass (left *y*-axis) of IgM ACPA 2D5 and anti-bt. The mean molecular mass of each peak is stated below each graph. The earlier a protein elutes, the higher its molecular mass. Shown are representative runs ($n = 2$). (B) Native PAGE (3–8% Tris-acetate) gel of different IgM monoclonals with and without J chain. Additional characterization can be found in Supplemental Fig. 1.

between the two isoforms remain more pronounced when tested on the CCP4 coat. For both Ags, we found that at lower Ag densities the hexameric isoform progressively activates complement more than the pentamer, so much so that at the lowest densities tested, activation was observed only for hexameric, but not for pentameric, IgM.

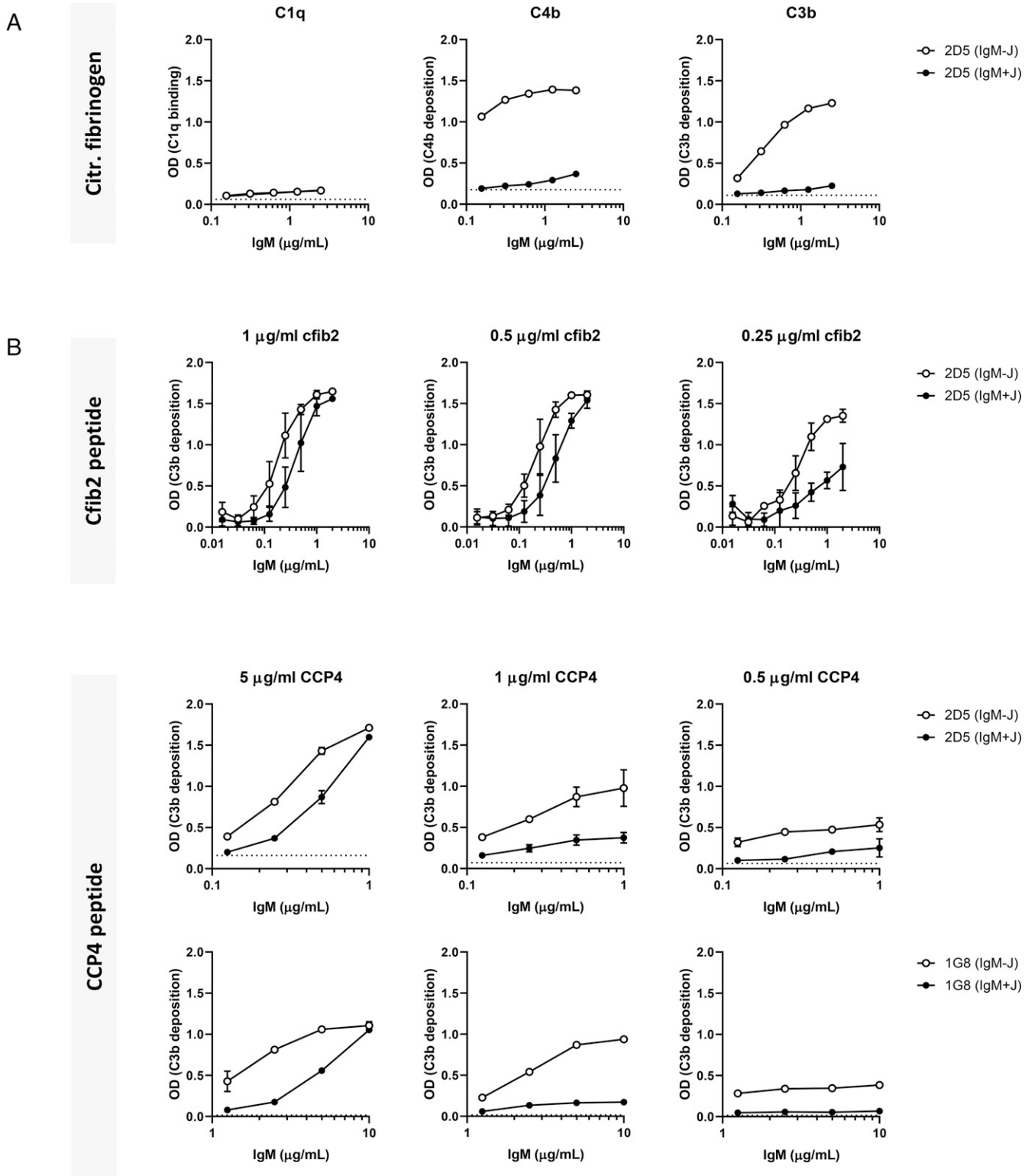


**FIGURE 3.** Complement activation by RA-specific IgM autoantibodies bound to different Ags. (**A**) Deposition of C1q, C4b, and C3b by IgM APCA 2D5 on citrullinated fibrinogen (10 μg/ml). Representative graphs are shown ($n \geq 2$). (**B**) C3b deposition by IgM ACPA 2D5 and ACPA 1G8 on varying concentrations of citrullinated peptides Cfib2 (2D5 only) and CCP4. Data are plotted as the mean ± SD of two technical duplicates within one experiment. Representative graphs are shown ($n = 4$).

We also extended our observations to a second clone, ACPA 1G8, which could activate complement on the synthetic CCP4 coat, whereas it was unable to do so when bound to citrullinated fibrinogen. In general, this clone is less potent than the ACPA 2D5. Again, the differences between the hexameric and pentameric IgM are more pronounced at lower Ag densities. Overall, this emphasizes that Ag density, but also the nature of the Ag, is an important

driver of complement activation by IgM. Sufficient Ag levels are especially important for pentameric IgM, which at high levels can activate complement to a similar extent as hexameric IgM.

*Complement activation by IgG1 and pentameric IgM, but not hexameric, is strongly dependent on Ag density*

We were surprised by the strong dependency of pentameric IgM on Ag density, and we set out to study this effect in more detail in a controlled system using Abs specific to bt. To control the Ag densities in this assay, we biotinylated HSA at different concentrations. We chose conditions mimicking low to relatively high Ag densities by biotinylating HSA at concentrations ranging from 15 to 120 μM, which we determined resulted in HSA with, respectively, 1–14 bts per molecule. The HSA-bt was used in a deposition ELISA to measure binding or deposition of C1q, C4b, and C3b (Fig. 1C).

As with the IgM ACPAs, we found almost no C1q binding to any of the Abs at the lowest Ag density (15 μM bt) we tested. With these conditions, however, pentameric IgM is able to activate complement sufficiently to cause C4b and C3b deposition, albeit less than IgM−J, despite equal binding of both isoforms to the coat (Supplemental Fig. 2A). As we increase the density of bt, the differences between pentameric and hexameric IgM become smaller (Fig. 4A). Although no C1q binding could be demonstrated, C3b deposition could be blocked to undetectable levels by inhibiting C1q, indicating the classical pathway as main driver for the C3b deposition. No C3b deposition was observed in the control condition, i.e., HSA without bt (Supplemental Fig. 3A, 3B).

When we compare complement activation by IgM with that by IgG1, we observed that at the lowest Ag densities IgG1 is, in contrast with IgM, not able to activate complement. For the high Ag density condition, we found that IgG1 was able to bind the most C1q, followed by hexameric and then pentameric IgM. Interestingly, this does not translate to more C4b or C3b deposition, which takes place to a similar extent for IgM and IgG1 at this Ag density.

Similar results were obtained at various dilutions of human serum (Supplemental Fig. 3C).

Next, we wished to confirm that the differences we found in classical pathway activation and C3b deposition are also reflected in terminal pathway activation and subsequent cell lysis. We measured the lytic activity of Abs in a CDC assay for which we biotinylated RBCs at varying concentrations of bt (7–125 μM) (Fig. 1D). Again, we found that hexameric causes relatively more lysis than pentameric IgM at the lowest Ag densities (7–15 μM bt), while IgG1 does not cause any lysis at these critical conditions. At higher Ag densities, we found that the differences between the Abs become smaller, whereas at the highest densities tested, all three Abs activate complement to a similar extent (Fig. 4B). In line with the data obtained in ELISA, we found similar results with various dilutions of human serum (Supplemental Fig. 3C).

Taken together, we show that Ag density is an important driver of classical and terminal pathway activation (Fig. 4C). Hexameric IgM is a more potent complement activator than pentameric IgM or IgG1, especially at low Ag densities. These differences are lost at higher densities.

*Proximity of Ag affects complement activation by IgM+J more than IgM−J*

Complement activation by IgG has been shown to be less efficient when it recognizes an Ag/epitope more distal from the cell (43). However, to our knowledge, this has never been shown for IgM. We therefore investigated the effect of the spatial arrangement of Ags on complement activation by IgM. We used three biotinylation reagents with different spacer arm lengths (Fig. 5A) and compared them in complement deposition and CDC assays as before.

In general, both IgM and IgG Abs induced less activation with longer linkers (Fig. 5B, 5C, Supplemental Fig. 2B, 2C). Furthermore, under these conditions, hexameric IgM was a better complement activator than pentameric IgM or IgG1. Overall, our data strongly indicate that both Ag density and distance from target surface are critical components determining the efficiency of complement deposition leading to CDC. In addition, fully hexameric IgM largely compensates for this, while pentameric IgM and IgG1 are less capable to do so under suboptimal conditions.

## Discussion

Recently, interest has increased with IgM after the discovery that pentameric IgM takes on a similar, hexagonal conformation to hexameric IgM both in solution and when it is in complex with Ag and C1 (10, 12–14). This appears to be at odds with previous findings showing that hexameric IgM is a more potent complement activator than pentameric IgM. Furthermore, reports on relative complement activating potencies of the two IgM isomers vary considerably across different studies (6). Together, these findings prompted us to conduct a more thorough investigation of complement activation by IgM. Our results clearly demonstrate that at low Ag densities, hexameric IgM (IgM−J) is a much more potent activator than pentameric IgM (IgM+J), while at high densities, they activate complement similarly.

Ag binding by Abs is the first step in the classical pathway and drives the conformational changes within the Ab necessary to activate complement. In solution, IgM is in a semiplanar, stellate conformation, and the residues within the IgM Cμ3 domain are shielded from recognition by C1q (11, 44). Several groups have studied the structure of the pentameric IgM-Fc using (cryo)electron microscopy and have found that it forms an asymmetric hexagon, in which the J chain takes up the place of a missing sixth arm resulting in a 50- to 60-degree gap (12–14). In the absence of J chain, IgM forms stable hexamers or more tightly packed pentamers to compensate for reduced structural stability (12).

On Ag binding, IgM changes its conformation to a nonplanar, dome shape to expose these residues so C1 can bind (11, 44). Sharp et al. (10) proposed that interactions within the IgM–C1 complex induce an overall hexagonal arrangement of the entire complex, and that the concerted compaction of C1q leads to rearrangement of the proteases within the complex to activate downstream complement mediators. The resulting C1–IgM complex is symmetric and hexagonal in arrangement, regardless of IgM's polymerization state. These interactions are strongly reminiscent of IgG–C1 complexes, for which preferably six IgG monomers interact with one C1q molecule and form hexamers on Ag binding (15, 16, 45). However, as the multiple IgM–Fc structures show, Ag binding is not a strict requirement for a hexagonal arrangement of IgM in solution; therefore, the differences in complement activation between pentameric and hexameric IgM cannot simply be explained by differences in conformation. Further insights into the dynamics of the pentameric and hexameric core may prove key to completely understanding the differences in complement activating potency.

With our set of matched humanized anti-bt Abs, we could further elaborate on the effect of Ag density on complement activation by hexameric and pentameric IgM, as well as IgG1. Besides a pronounced difference in activity of hexameric versus pentameric IgM depending on Ag density, there exists an even stronger dependency on Ag density for human IgG1. This is in line with what has been shown previously in several other, nonhuman systems (46, 47). To activate complement, IgG forms

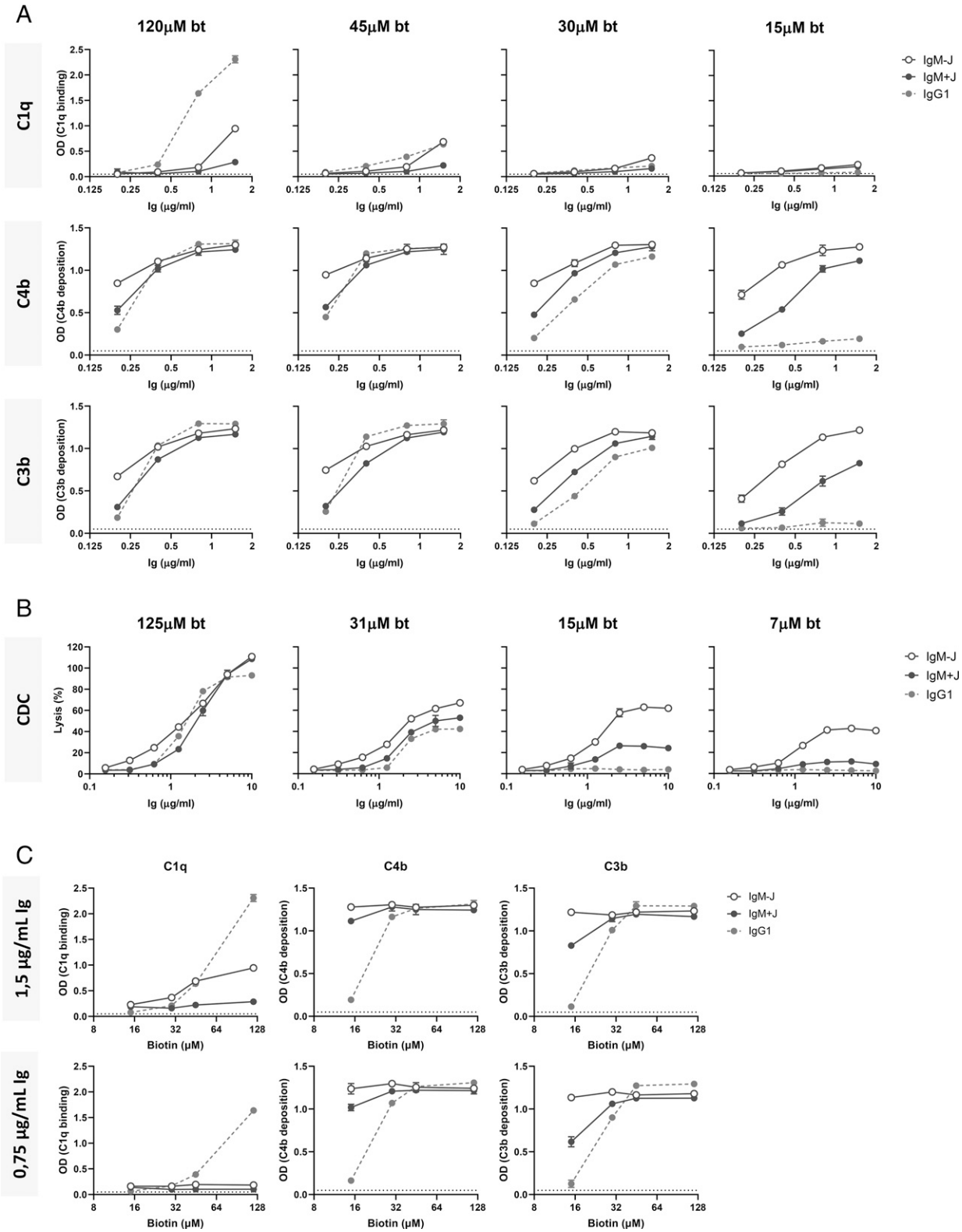


**FIGURE 4.** The effect of Ag density on complement activation by IgM. Classical and terminal pathway activation (see Fig. 1C and 1D for setup) induced by a matched set of anti-bt antibodies (IgM+J, IgM−J, and IgG1) with varying Ag densities. (**A**) C1q, C4b, and C3b deposition induced by anti-bt antibodies as measured in ELISA on HSA-bt biotinylated at varying concentrations of bt (15, 30, 45, and 120 μM). Representative graphs are shown ($n = 3$). (**B**) Complement-mediated lysis by anti-bt antibodies of RBCs that were biotinylated at varying concentrations of bt (7, 15, 31, and 125 μM). All data represent the mean ± SD of two technical duplicates within one experiment. Representative graphs are shown ($n = 3$). (**C**) Complement deposition at different Ag densities for 1.5 and 0.75 μg/ml Ab [data from (A) replotted].

oligomers through reversible Fc–Fc interactions on Ag binding, but only if there is both enough Ag and Ab present for monomers to interact (48, 49). This is reflected in our experiments, because at the lowest densities tested, IgG1 does not activate complement. Interestingly, we found more C1q bound to IgG1 than to IgM at the highest densities, but this did not translate

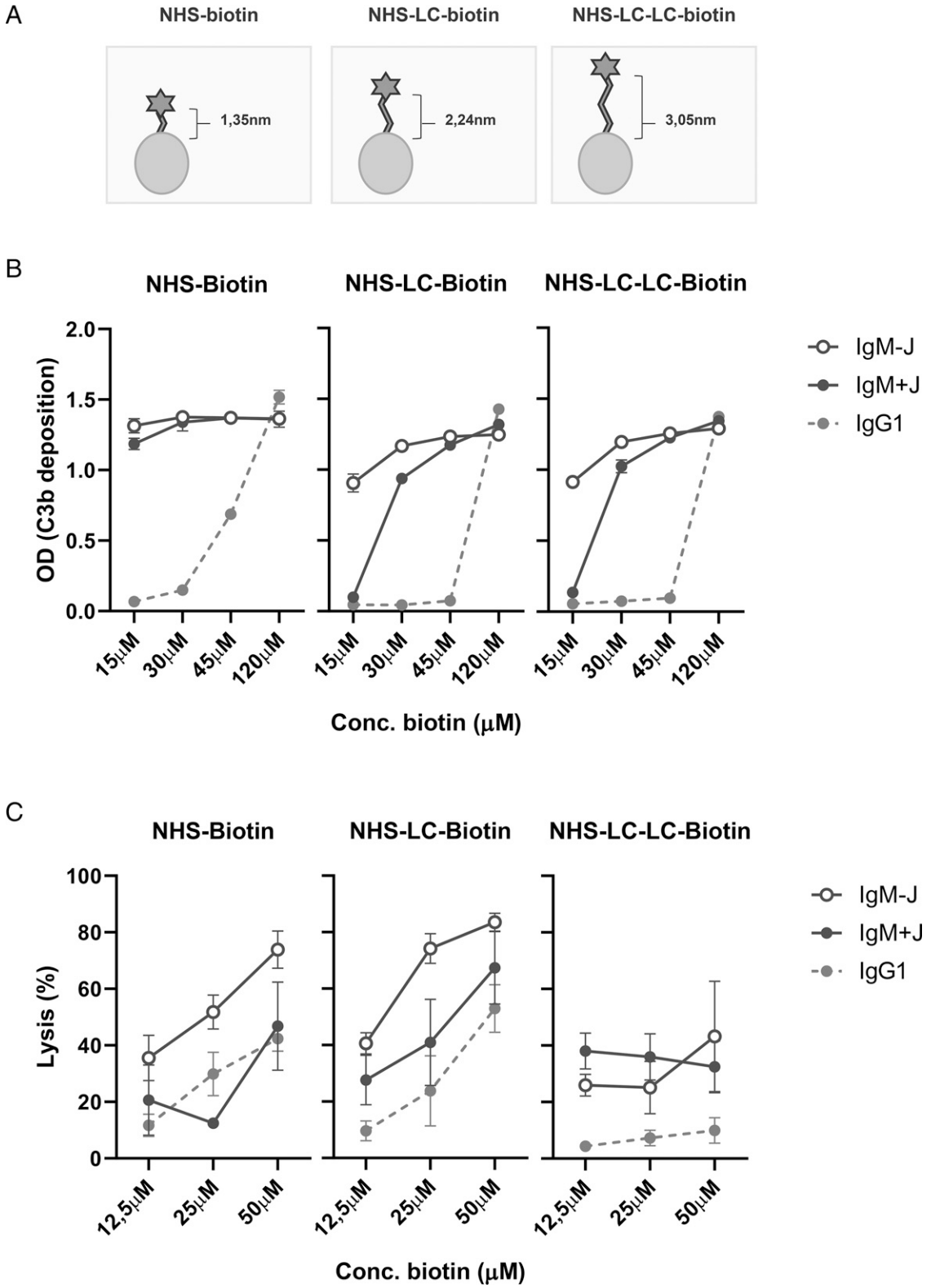


**FIGURE 5.** IgM complement activation is affected by Ag proximity. (**A**) Schematic representation of HSA-bt, containing bt with spacer arms of varying lengths. (**B**) Deposition of C3b by anti-bt antibodies (0.75 μg/ml) on HSA-bt at varying concentrations of NHS-bt, NHS-LC-bt, and NHS-LC-LC-bt (15, 30, 45, and 120 μM). Data are plotted as the mean ± SD of two technical duplicates within one experiment. (**C**) CDC induced by anti-bt antibodies (5 μg/ml) of RBCs biotinylated with varying concentrations of NHS-bt, NHS-LC-bt, and NHS-LC-LC-bt (12.5, 25, and 50 μM). Data are plotted as the mean and SD of two technical duplicates within two experiments. Representative graphs are shown (C3b deposition: $n = 3$, CDC: $n = 2–5$).

into more C4b/C3b deposition and terminal pathway activation. This phenomenon has recently also been described for complement activation by IgG2, which is able to induce lysis but shows very little C1q binding when compared with IgG1 (50). It was found that the C1–IgG complex can be either stabilized by efficient hexamer formation or by interactions between C1q and the proteases

C1r/C1s. Measured C1q is not necessarily complexed with its proteases and therefore does not always correlate with downstream complement activation.

Next to Ag density, the nature of the Ag (i.e., distance from membrane, membrane fluidity) and of Ag–Ab interactions (i.e., affinity, binding epitope) also affect complement activation (51). We found that the effects of Ag density we observed could be extended to multiple clones and reactivities. The differences we observed between the two ACPA clones are likely to stem from their different binding affinities toward the citrullinated Ags, because the 2D5 clone appears to be able to bind with higher affinity than the 1G8 clone (31). Furthermore, we also showed that hexameric IgM activates complement better with more distal Ags when compared with pentameric IgM and even more so when compared with IgG1. It was previously shown that CDC by IgG becomes less effective the further an epitope is removed from the cell surface (43), and IgM complement activation is affected in a similar manner, albeit to a lesser extent. Interestingly, we find that C3b deposition by hexameric IgM is similar in all conditions tested. However, it is likely that at least part of this deposition did not occur directly at the cell surface, but rather at structures slightly farther removed, and this deposition would therefore probably not contribute to formation of the membrane attack complex.

We found that the preparation of purified IgM is also crucial. Several previous studies made use of the CH12 murine lymphoma cell line that produced both hexameric and pentameric IgM in a 50/50 manner and is specific for the hapten trinitrophenyl (24, 25, 52). It coexpresses low amounts of J chain, which causes it to produce both isoforms, which are technically difficult to separate. It is likely that these studies were instead performed with mixtures of isoforms. We also found that harsh elution conditions (i.e., acidic elution) during IgM purification can lead to aggregation, especially in the case of hexameric IgM, because in our hands, this polymer is not as stable as the J chain–containing pentamer and easily aggregates/precipitates. In this study, we used a transient transfection system that allowed us full control over J chain coexpression, in combination with a very mild purification protocol to produce well-defined, homogeneous IgM preparations.

Lastly, the biological relevance of hexameric IgM remains uncertain. It has mainly been found in different (B cell–driven) pathologies and in cell culture systems. IgMs isolated from patients with Waldenström's macroglobulinemia (24, 53, 54), reoccurring bacterial unitary tract infections (55), and cold agglutinin disease (24) have been shown to lack J chain and form hexamers. For the latter, enhanced hemolytic activity was demonstrated for hexameric versus pentameric autoantibodies against RBC Ag Ii. In the case of IgM gammopathies, symptoms related to the monoclonal IgM depend on the type and specificity of the monoclonal (i.e., cryoglobulin, anti-RBC autoantibody), but may also be determined by the polymerization state of IgM. Furthermore, raised hexameric IgM was observed after specific immunization in patients with recurrent lower urinary tract infections, which was associated with nonresponse (55). Regardless, the extent of J chain deficiency within these, but also other disorders, remains largely unexplored. Additional studies to map the prevalence of hexameric IgM in IgM-driven pathologies and diseases that present with IgM autoantibodies such as rheumatoid arthritis could provide valuable insights to better understand the pathogenic role of IgM.

In vitro, some EBV-transformed B cells were found to also secrete IgM without J chain (56). In mice, B cell lymphomas and hybridomas have been found to secrete both J chain–positive and –negative IgM (6, 22, 23, 25, 57), and this composition can be altered by stimulation with LPS or IL-5 (24, 52). These studies overall find that the majority of IgMs without J chain are secreted as hexamers, but the composition of polymers appears to depend strongly on the expression system used. Furthermore, purification of hexameric IgM from serum has been reported (58). However, our own attempts to separate serum IgM from healthy individuals into fractions with and without J chain did yield J chain–negative IgM, but this appeared to be of similar or smaller size to pentameric IgM (data not shown). Although this does not rule out the possibility that hexameric IgM plays a role in normal immunity, we think it unlikely that it is present in large quantities in healthy individuals during homeostasis. Because it is such a potent complement activator, it could also potentially be very dangerous to have high levels of hexameric IgM in circulation. Possibly, its appearance is restricted to situations in relation to pathology.

Overall, we have shown that the relative differences in complement activation by hexameric and pentameric IgM are in part subject to Ag binding. The Ag density, but also the nature of the Ag, i.e., its distance from the membrane, determine the activating potency of Abs. This affects hexameric IgM the least, which at critical Ag conditions steadily outcompetes both pentameric IgM and, even more so, IgG1. This highlights the importance of IgM in complement activation, because we find that in circumstances with critical Ag conditions, it is a more potent complement activator than IgG.

## Acknowledgments

We thank Charlotte Nurmohamed for help with performing ELISAs and Jana Koers for valuable input.

## Disclosures

The authors have no financial conflicts of interest.

## References

1. Blandino, R., and N. Baumgarth. 2019. Secreted IgM: new tricks for an old molecule. *J. Leukoc. Biol.* 106: 1021–1034.
2. Anelli, T., and E. van Anken. 2013. Missing links in antibody assembly control. *Int. J. Cell Biol.* 2013: 606703.
3. Keyt, B. A., R. Baliga, A. M. Sinclair, S. F. Carroll, and M. S. Peterson. 2020. Structure, function, and therapeutic use of IgM antibodies. *Antibodies (Basel)* 9: 53.
4. Azuma, Y., Y. Ishikawa, S. Kawai, T. Tsunenari, H. Tsunoda, T. Igawa, S. Iida, M. Nanami, M. Suzuki, R. F. Irie, et al. 2007. Recombinant human hexamer-dominant IgM monoclonal antibody to ganglioside GM3 for treatment of melanoma. *Clin. Cancer Res.* 13: 2745–2750.
5. Cattaneo, A., and M. S. Neuberger. 1987. Polymeric immunoglobulin M is secreted by transfectants of non-lymphoid cells in the absence of immunoglobulin J chain. *EMBO J.* 6: 2753–2758.
6. Collins, C., F. W. Tsui, M. J. Shulman, Q. Yu, M. L. Cowan, L. Feigenbaum, P. E. Love, and A. Singer. 2002. Differential activation of human and guinea pig complement by pentameric and hexameric IgM. *Eur. J. Immunol.* 32: 1802–1810.
7. Niles, M. J., L. Matsuuchi, and M. E. Koshland. 1995. Polymer IgM assembly and secretion in lymphoid and nonlymphoid cell lines: evidence that J chain is required for pentamer IgM synthesis. *Proc. Natl. Acad. Sci. USA* 92: 2884–2888.
8. Poon, P. H., M. L. Phillips, and V. N. Schumaker. 1985. Immunoglobulin M possesses two binding sites for complement subcomponent C1q, and soluble 1:1 and 2:1 complexes are formed in solution at reduced ionic strength. *J. Biol. Chem.* 260: 9357–9365.
9. Sørensen, V., I. B. Rasmussen, V. Sundvold, T. E. Michaelsen, and I. Sandlie. 2000. Structural requirements for incorporation of J chain into human IgM and IgA. *Int. Immunol.* 12: 19–27.
10. Sharp, T. H., A. L. Boyle, C. A. Diebolder, A. Kros, A. J. Koster, and P. Gros. 2019. Insights into IgM-mediated complement activation based on in situ structures of IgM-C1-C4b. *Proc. Natl. Acad. Sci. USA* 116: 11900–11905.
11. Czajkowsky, D. M., and Z. Shao. 2009. The human IgM pentamer is a mushroom-shaped molecule with a flexural bias. *Proc. Natl. Acad. Sci. USA* 106: 14960–14965.
12. Hiramoto, E., A. Tsutsumi, R. Suzuki, S. Matsuoka, S. Arai, M. Kikkawa, and T. Miyazaki. 2018. The IgM pentamer is an asymmetric pentagon with an open groove that binds the AIM protein. *Sci. Adv.* 4: eaau1199.
13. Li, Y., G. Wang, N. Li, Y. Wang, Q. Zhu, H. Chu, W. Wu, Y. Tan, F. Yu, X. D. Su, N. Gao, and J. Xiao. 2020. Structural insights into immunoglobulin M. *Science* 367: 1014–1017.
14. Kumar, N., C. P. Arthur, C. Ciferri, and M. L. Matsumoto. 2021. Structure of the human secretory immunoglobulin M core. *Structure* 29: 564–571.e3.
15. Diebolder, C. A., F. J. Beurskens, R. N. de Jong, R. I. Koning, K. Strumane, M. A. Lindorfer, M. Voorhorst, D. Ugurlar, S. Rosati, A. J. R. Heck, et al. 2014. Complement is activated by IgG hexamers assembled at the cell surface. *Science* 343: 1260–1263.

16. Wang, G., R. N. de Jong, E. T. van den Bremer, F. J. Beurskens, A. F. Labrijn, D. Ugurlar, P. Gros, J. Schuurman, P. W. Parren, and A. J. Heck. 2016. Molecular basis of assembly and activation of complement component C1 in complex with immunoglobulin G1 and antigen. *Mol. Cell* 63: 135–145.
17. Pluschke, G., G. Bordmann, M. E. Daoudaki, J. D. Lambris, M. Achtman, and M. Neibert. 1989. Isolation of rat IgM to IgG hybridoma isotype switch variants and analysis of the efficiency of rat Ig in complement activation. *Eur. J. Immunol.* 19: 131–135.
18. Brüggemann, M., G. T. Williams, C. I. Bindon, M. R. Clark, M. R. Walker, R. Jefferis, H. Waldmann, and M. S. Neuberger. 1987. Comparison of the effector functions of human immunoglobulins using a matched set of chimeric antibodies. J. Exp. Med. 166: 1351–1361.
19. Michaelsen, T. E., Ø. Ihle, K. J. Beckstrøm, T. K. Herstad, J. Kolberg, E. A. Høiby, and A. Aase. 2003. Construction and functional activities of chimeric mouse-human immunoglobulin G and immunoglobulin M antibodies against the *Neisseria meningitidis* PorA P1.7 and P1.16 epitopes. *Infect. Immun.* 71: 5714–5723.
20. Taylor, B., J. F. Wright, S. Arya, D. E. Isenman, M. J. Shulman, and R. H. Painter. 1994. C1q binding properties of monomer and polymer forms of mouse IgM mu-chain variants. Pro544Gly and Pro434Ala. *J. Immunol.* 153: 5303–5313.
21. Davis, A. C., and M. J. Shulman. 1989. IgM—molecular requirements for its assembly and function. *Immunol. Today* 10: 118–122, 127–128.
22. Davis, A. C., K. H. Roux, and M. J. Shulman. 1988. On the structure of polymeric IgM. *Eur. J. Immunol.* 18: 1001–1008.
23. Wiersma, E. J., C. Collins, S. Fazel, and M. J. Shulman. 1998. Structural and functional analysis of J chain-deficient IgM. *J. Immunol.* 160: 5979–5989.
24. Hughey, C. T., J. W. Brewer, A. D. Colosia, W. F. Rosse, and R. B. Corley. 1998. Production of IgM hexamers by normal and autoimmune B cells: implications for the physiologic role of hexameric IgM. *J. Immunol.* 161: 4091–4097.
25. Randall, T. D., L. B. King, and R. B. Corley. 1990. The biological effects of IgM hexamer formation. *Eur. J. Immunol.* 20: 1971–1979.
26. Hack, C. E., J. Paardekooper, R. J. Smeenk, J. Abbink, A. J. Eerenberg, and J. H. Nuijens. 1988. Disruption of the internal thioester bond in the third component of complement (C3) results in the exposure of neodeterminants also present on activation products of C3. An analysis with monoclonal antibodies. *J. Immunol.* 141: 1602–1609.
27. Leito, J. T. D., A. J. M. Ligtenberg, M. van Houdt, T. K. van den Berg, and D. Wouters. 2011. The bacteria binding glycoprotein salivary agglutinin (SAG/gp340) activates complement via the lectin pathway. *Mol. Immunol.* 49: 185–190.
28. McGrath, F. D. G., M. C. Brouwer, G. J. Arlaud, M. R. Daha, C. E. Hack, and A. Roos. 2006. Evidence that complement protein C1q interacts with C-reactive protein through its globular head region. *J. Immunol.* 176: 2950–2957.
29. Bagçi, H., F. Kohen, U. Kusçuoglu, E. A. Bayer, and M. Wilchek. 1993. Monoclonal anti-biotin antibodies simulate avidin in the recognition of biotin. *FEBS Lett.* 322: 47–50.
30. Kohen, F., H. Bagci, G. Barnard, E. A. Bayer, B. Gayer, D. G. Schindler, E. Ainbinder, and M. Wilchek. 1997. Preparation and properties of anti-biotin antibodies. *Methods Enzymol.* 279: 451–463.
31. Reijm, S., T. Kissel, G. Stoeken-Rijsbergen, L. M. Slot, C. M. Wortel, H. J. van Dooren, N. E. W. Levarht, A. S. B. Kampstra, V. F. A. M. Derksen, P. O. Heer, et al. 2021. Cross-reactivity of IgM anti-modified protein antibodies in rheumatoid arthritis despite limited mutational load. *Arthritis Res. Ther.* 23: 230.
32. de Lange, G. G., A. M. van Leeuwen, A. Vlug, P. H. van Eede, C. P. Engelfriet, and P. J. Lincoln. 1989. Monoclonal antibodies against IgG allotypes G1m(z), G1m(a), G1m(f), G3m(b1/u) and G3m(g1): their usefulness in HAI and capture ELISA. *Exp. Clin. Immunogenet.* 6: 18–30.
33. Duquerroy, S., E. A. Stura, S. Bressanelli, S. M. Fabiane, M. C. Vaney, D. Beale, M. Hamon, P. Casali, F. A. Rey, B. J. Sutton, and M. J. Taussig. 2007. Crystal structure of a human autoimmune complex between IgM rheumatoid factor RF61 and IgG1 Fc reveals a novel epitope and evidence for affinity maturation. *J. Mol. Biol.* 368: 1321–1331.
34. Sohi, M. K., A. L. Corper, T. Wan, M. Steinitz, R. Jefferis, D. Beale, M. He, A. Feinstein, B. J. Sutton, and M. J. Taussig. 1996. Crystallization of a complex between the Fab fragment of a human immunoglobulin M (IgM) rheumatoid factor (RF-AN) and the Fc fragment of human IgG4. *Immunology* 88: 636–641.
35. Falkenburg, W. J. J., A. C. Kempers, G. Dekkers, P. Ooijevaar-de Heer, A. E. H. Bentlage, G. Vidarsson, D. van Schaardenburg, R. E. M. Toes, H. U. Scherer, and T. Rispens. 2017. Rheumatoid factors do not preferentially bind to ACPA-IgG or IgG with altered galactosylation. *Rheumatology (Oxford)* 56: 2025–2030.
36. Falkenburg, W. J. J., N. Oskam, J. Koers, L. van Boheemen, P. Ooijevaar-de Heer, G. M. Verstappen, H. Bootsma, F. G. M. Kroese, D. van Schaardenburg, G. Wolbink, and T. Rispens. 2020. Identification of clinically and pathophysiologically relevant rheumatoid factor epitopes by engineered IgG targets. *Arthritis Rheumatol.* 72: 2005–2016.
37. Zimm, B. H. 1948. The scattering of light and the radial distribution function of high polymer solutions. *J. Chem. Phys.* 16: 1093–1099.
38. Hawe, A., W. Friess, M. Sutter, and W. Jiskoot. 2008. Online fluorescent dye detection method for the characterization of immunoglobulin G aggregation by size exclusion chromatography and asymmetrical flow field flow fractionation. *Anal. Biochem.* 378: 115–122.
39. Rispens, T., and P. Ooijevaar-de Heer. 2016. Quantification of the degree of biotinylation of proteins using proteinase K digestion and competition ELISA. *J. Immunol. Methods* 430: 61–63.
40. Dekkers, G., L. Treffers, R. Plomp, A. E. H. Bentlage, M. de Boer, C. A. M. Koeleman, S. N. Lissenberg-Thunnissen, R. Visser, M. Brouwer, J. Y. Mok, et al. 2017. Decoding the human immunoglobulin G-glycan repertoire reveals a spectrum of Fc-receptor- and complement-mediated-effector activities. *Front. Immunol.* 8: 877.
41. van de Stadt, L. A., P. A. van Schouwenburg, S. Bryde, S. Kruithof, D. van Schaardenburg, D. Hamann, G. Wolbink, and T. Rispens. 2013. Monoclonal anti-citrullinated protein antibodies selected on citrullinated fibrinogen have distinct targets with different cross-reactivity patterns. *Rheumatology (Oxford)* 52: 631–635.
42. Kissel, T., S. Reijm, L. M. Slot, M. Cavallari, C. M. Wortel, R. D. Vergroesen, G. Stoeken-Rijsbergen, J. C. Kwekkeboom, A. Kampstra, E. Levarht, et al. 2020. Antibodies and B cells recognising citrullinated proteins display a broad cross-reactivity towards other post-translational modifications. *Ann. Rheum. Dis.* 79: 472–480.
43. Cleary, K. L. S., H. T. C. Chan, S. James, M. J. Glennie, and M. S. Cragg. 2017. Antibody distance from the cell membrane regulates antibody effector mechanisms. *J. Immunol.* 198: 3999–4011.
44. Müller, R., M. A. Gräwert, T. Kern, T. Madl, J. Peschek, M. Sattler, M. Groll, and J. Buchner. 2013. High-resolution structures of the IgM Fc domains reveal principles of its hexamer formation. *Proc. Natl. Acad. Sci. USA* 110: 10183–10188.
45. Ugurlar, D., S. C. Howes, B. J. de Kreuk, R. I. Koning, R. N. de Jong, F. J. Beurskens, J. Schuurman, A. J. Koster, T. H. Sharp, P. W. H. I. Parren, and P. Gros. 2018. Structures of C1-IgG1 provide insights into how danger pattern recognition activates complement. *Science* 359: 794–797.
46. Borsos, T., R. M. Chapuis, and J. J. Langone. 1981. Distinction between fixation of C1 and the activation of complement by natural IgM anti-hapten antibody: effect of cell surface hapten density. *Mol. Immunol.* 18: 863–868.
47. Kratz, H. J., T. Borsos, and H. Isliker. 1985. Mouse monoclonal antibodies at the red cell surface—II. Effect of hapten density on complement fixation and activation. *Mol. Immunol.* 22: 229–235.
48. Strasser, J., R. N. de Jong, F. J. Beurskens, J. Schuurman, P. W. H. I. Parren, P. Hinterdorfer, and J. Preiner. 2020. Weak fragment crystallizable (Fc) domain interactions drive the dynamic assembly of IgG oligomers upon antigen recognition. *ACS Nano* 14: 2739–2750.
49. Strasser, J., R. N. de Jong, F. J. Beurskens, G. Wang, A. J. R. Heck, J. Schuurman, P. W. H. I. Parren, P. Hinterdorfer, and J. Preiner. 2019. Unraveling the macromolecular pathways of IgG oligomerization and complement activation on antigenic surfaces. *Nano Lett.* 19: 4787–4796.
50. Zwarthoff, S. A., K. Widmer, A. Kuipers, J. Strasser, M. Ruyken, P. C. Aerts, C. J. C. de Haas, D. Ugurlar, M. A. den Boer, G. Vidarsson, et al. 2021. C1q binding to surface-bound IgG is stabilized by $C1r_2s_2$ proteases. *Proc. Natl. Acad. Sci. USA* 118: e2102787118.
51. Pedersen, M. B., X. Zhou, E. K. U. Larsen, U. S. Sørensen, J. Kjems, J. V. Nygaard, J. R. Nyengaard, R. L. Meyer, T. Boesen, and T. Vorup-Jensen. 2010. Curvature of synthetic and natural surfaces is an important target feature in classical pathway complement activation. *J. Immunol.* 184: 1931–1945.
52. Randall, T. D., R. M. E. Parkhouse, and R. B. Corley. 1992. J chain synthesis and secretion of hexameric IgM is differentially regulated by lipopolysaccharide and interleukin 5. *Proc. Natl. Acad. Sci. USA* 89: 962–966.
53. Eskeland, T., and T. B. Christensen. 1975. IgM molecules with and without J chain in serum and after purification, studied by ultracentrifugation, electrophoresis, and electron microscopy. *Scand. J. Immunol.* 4: 217–228.
54. Petrušić, V., I. Zivković, M. Stojanović, I. Stojićević, E. Marinković, A. Inić-Kanada, and L. Dimitijević. 2011. Antigenic specificity and expression of a natural idiotope on human pentameric and hexameric IgM polymers. *Immunol. Res.* 51: 97–107.
55. Petrušić, V., M. Stojanović, I. Zivković, A. Inić-Kanada, and L. Dimitrijević. 2010. Changes in composition of IgM polymers in patients suffering from recurrent urinary bacterial infections after bacterial immunization treatment. *Immunol. Invest.* 39: 781–795.
56. Meng, Y. G., A. B. Criss, and K. E. Georgiadis. 1990. J chain deficiency in human IgM monoclonal antibodies produced by Epstein-Barr virus-transformed B lymphocytes. *Eur. J. Immunol.* 20: 2505–2508.
57. Parkhouse, R. M., B. A. Askonas, and R. R. Dourmashkin. 1970. Electron microscopic studies of mouse immunoglobulin M; structure and reconstitution following reduction. *Immunology* 18: 575–584.
58. Michaelsen, T. E., S. Emilsen, R. H. Sandin, B. K. Granerud, D. Bratlie, O. Ihle, and I. Sandlie. 2017. Human secretory IgM antibodies activate human complement and offer protection at mucosal surface. *Scand. J. Immunol.* 85: 43–50.